Bioactive Materials 5 (2020) 192–200

Contents lists available at ScienceDirect

Bioactive Materials

journal homepage: http://www.keaipublishing.com/biomat

Tuning C–C sp2/sp3 ratio of DLC films in FCVA system for biomedical application

Xi Rao[a,b,*], Jihan Yang[a,b], Zilin Chen[a,b], Yidie Yuan[a,b], Qiubing Chen[a,b], Xue Feng[c], Lizhao Qin[a], Yongping Zhang[a,b,**]

[a] Key Laboratory of Luminescent and Real-Time Analytical Chemistry (Southwest University), Ministry of Education, School of Materials and Energy, Southwest University, Chongqing, 400715, PR China
[b] Chongqing Key Laboratory of Soft-Matter Material Chemistry and Function Manufacturing, Southwest University, Chongqing, 400715, PR China
[c] Department of Clinical Laboratory, University-Town Hospital of Chongqing Medical University, Chongqing, 401331, PR China

ARTICLE INFO

Keywords:
DLC film
FCVA system
Apatite formation
Hemolysis
Cytotoxicity

ABSTRACT

Diamond like carbon (DLC) films with different C–C sp2/sp3 ratios were prepared by tuning the N2 flow rate in a filtered cathodic vacuum arc (FCVA) system. The increase of N2 flow rate facilitated the increase of C–C sp2/sp3 ratio (1.09–2.66), the growth of particle size (0.78–1.58 nm) and the improvement of surface roughness. The SBF immersion results, as well as WCAs (77.57°~71.71°), hemolysis rate (0.14–1.00%) and cytotoxicity level (0) demonstrated that the as-fabricated DLC film was promising for biomedical application. As a result of surface charge effect, the apatite layers formed in the SBF increased with the increase of C–C sp2/sp3 ratio until 1.74 and then showed a tiny decrease during 1.74–2.66. A raise of hemolysis and cytotoxicity was observed when sp2/sp3 ratio was increased. Moreover, a decrease of friction coefficient of Si surface induced by increasing sp2/sp3 ratio was respectively evidenced in ambient air and SBF lubrication environments.

1. Introduction

One of the most efficient ways to surgically treat on osteoarthritis is the joint replacement. However, the premature implantation failure occurs due to excessive wear and corrosion, which is always companied with osteolysis and aseptic loosening [1–3]. Thus, one of the most enormous challenges of joint replacement lies in the enhancement of implants' abrasive resistance. The diamond like carbon (DLC) films have shown excellent wear resistance, high hardness and low friction coefficient [4–6], hence it could be potentially used for modifying the surface of joint implants. Concerning recent reports, such films deposited using different methods could improve the tribological property [7], the biocompatibility [8,9], or even the bactericidal ability [10,11]. The DLC films are mainly consisted of a combination of four-fold coordinated sp3 sites, as in diamond; and the three-fold coordinated sp2 sites, as in graphite. Thus, the bonds structure fraction of sp2/sp3 could not only affect the film's tribological properties, but also influence the surface biological responses *e.g.* osteoblastogenesis, fibroblastic response, inflammatory reactions and so on. Wei et al. showed the C–C sp^2/sp^3 ratio of DLC film could obviously affect its biocompatibility [12]. Dorner et al. [13] indicated the content of C–C sp^2 in DLC film benefited in mouse fibroblasts differentiation. In spite that many researches proved the DLC films can be used to improve the tribological properties of orthopaedical implants [14], few scholars focused on the osteogenesis of DLC film *in vivo* or *in vitro* [15]. Furthermore, the influence of C–C bonds structure fraction on the DLC film's osteogenesis ability as well as other biomedical properties has been seldomly reported.

Conventionally, the DLC films are deposited using chemical vapor deposition (CVD) methods or physical vapor deposition (PVD) methods. Among these techniques, plasma assisted deposition is one of the most widespread approaches, which could deposit high quality DLC film at a considerably low temperature in vacuum atmosphere [16]. As a kind of plasma assisted deposition techniques, filtered cathodic vacuum arc (FCVA) technique exhibits unique properties *e.g.* high ion energy, high ionization rate and multiple ion charge states, for the production of

Peer review under responsibility of KeAi Communications Co., Ltd.
* Corresponding author. Key Laboratory of Luminescent and Real-Time Analytical Chemistry (Southwest University), Ministry of Education, School of Materials and Energy, Southwest University, Chongqing, 400715, PR China.
** Corresponding author. Key Laboratory of Luminescent and Real-Time Analytical Chemistry (Southwest University), Ministry of Education, School of Materials and Energy, Southwest University, Chongqing, 400715, PR China.
E-mail addresses: raoxiemail@swu.edu.cn (X. Rao), zhangyyping@yahoo.com (Y. Zhang).

https://doi.org/10.1016/j.bioactmat.2020.02.009
Received 6 December 2019; Received in revised form 9 February 2020; Accepted 11 February 2020

hard films, *e.g.* tetrahedral amorphous carbon film and DLC film [17]. Moreover, the bonds structure fraction of DLC film could be easily adjusted by changing parameters of plasma system. For instance, the C–C sp2/sp3 ratio of the DLC film could be tuned by varying nitrogen flow during deposition [18–20].

In this study, we aimed to tune the C–C bonds structure of the DLC films and investigate its influence on the film's biomedical and tribological properties. The DLC films with different C–C sp2/sp3 ratio were deposited on the Si wafers in a homemade FCVA system by varying N2 flow rate. Subsequently, the biomedical properties *e.g.* bone bioactivity, hydrophilicity, hemocompatibility and cytocompatibility and the tribological property were evaluated to recognize the influence of C–C sp2/sp3 ratio.

2. Experimental procedures

2.1. DLC film preparation

The (100) n-type single crystalline silicon wafers were ultrasonically cleaned in acetone and ethanol for 10 min, respectively. Then, the substrates were placed in a FCVA system for DLC film deposition. The details of FCVA system were described elsewhere [21].

A cathodic arc source with a filter was used to produce carbon plasma from a graphite cathode of 99.99% purity. The cathodic arc source was operated at a direct current of 110 A. The unwanted neutral and macroparticles were removed by two 45° bent magnetic filter ducts. The system base pressure was 10 − 5 Pa. The DLC films were deposited on Si wafers at a constant negative bias voltage of 300 V. Before deposition the carbon was pre-implanted in substrate at 10 kV for 3 min to get a carbon transition layer, which could enhance the DLC films adherence to the substrate. In order to adjust the bonds structure of DLC films, the flow rate of the N2 was changed in the range of 0–20 sccm.

2.2. Tribological test

The tribological performance of the DLC films was investigated with the CSM tribometer (pin-on-disk) in the reciprocatory motion mode by applying samples in ambient air and SBF lubrication, respectively. Aluminum oxide balls with a diameter of 6 mm were used as the counterparts. The load of 1 N was kept for 2000 s at a revolving speed of 600 r/min, and the radius was 2.5 mm. The maximum contact pressure was approximately 1.5 GPa from the Hertz model for a ball on a flat surface. All the sliding tests were performed at ambient temperature of 20 ˚C and relative humidity of 20–30%. Each test was repeated three times with a variable coefficient of friction within 0.005.

2.3. Hydrophilicity test

The hydrophilicity of surface was evaluated by testing water contact angles (WCAs) on sample surfaces. A contact angle goniometer (JC2000D, China) was used for the investigation. A droplet (2 μL) of deionized water was put onto the sample surface to measure the contact angle. More than three samples were tested to obtain the average values along with the standard deviation.

2.4. SBF immersion

The osteogenesis of as-deposited DLC films was evaluated using a simulated body fluid immersion test. The DLC films with different sp2/sp3 ratio were immersed in SBF for 3, 7, 14 and 28 d. For each immersion duration, three samples with each kind of the films were employed. The SBF solution was prepared according to Kokubo and Takadam by dissolving reagent-grade chemicals (NaCl, NaHCO3, KCl, K2HPO4·3H2O, MaCl2·6H2O, CaCl2 and Na2SO4) in distilled water, and buffered at pH = 7.4 with tris-hydroxymethyl-aminomethane and HCl at 36.5 ˚C [22]. The ion concentrations (mM) of the SBF solution were 142 Na+, 5 K+, 1.5 Mg2 +, 2.5 Ca2 +, 147.8 Cl−, 4.2 HCO3–, 1 HPO42 − and 0.5 SO42 −, nearly equal to those of human blood plasma. Each sample was immersed in a plastic vial containing 50 mL of SBF and was kept under static conditions inside a biological thermostat at 37 ± 0.5 ˚C. The SBF was refreshed as the solution in vial was replaced by newly prepared SBF every two days, so that the lack of ions would not inhibit the apatite formation. In the present days, the samples were removed from the SBF, rinsed with distilled water and then air dried.

2.5. Hemolysis test

The mouse blood was collected in vacuum blood collection tube with K2EDTA. Then red blood cells (RBCs) were separated, purified and diluted for the volume ratio to 2% with PBS. The untreated silicon wafers and the wafers deposited with DLC film of various C–C sp2/sp3 ratio were respectively incubated with RBC at 37 ˚C for 1 h. The absorbance of the supernatants from each sample was measured using a microplate reader at 570 nm. The untreated RBCs were used as a negative control, the RBCs treated with 1% Triton X-100 were used as a positive control. The hemolysis rate was calculated using followed equation:

$$Hemolysis\ rate(\%) = \frac{OD_S - OD_N}{OD_P - OD_N} \times 100\% \quad (1)$$

Where the ODS is the optical density of the samples (untreated silicon wafer, DLC film deposited wafer), ODN is the optical density of negative controls, ODP is the optical density of positive controls.

2.6. Cytotoxicity test

Cell viability on the DLC films was assessed using the 3-(4, 5-dimethylthiazol-2-yl)-2, 5-diphenylterazolium bromide (MTT) assay (Beyotime Biotechnology, MTT Cell Proliferation and Cytotoxicity Assay Kit, C0009). A cell concentration of 105 cells/mL was seeded on the samples. The human epithelial cell line (HEK293T) was purchased from Cell Bank of Chinese Academy of Sciences, Shanghai. The HEK293T cells were seeded in 24-well plates at a density of 1 × 104 cells per well. After incubation overnight, cells were co-incubated with untreated silicon wafers and DLC film deposited wafers for 1, 3 and 7 days. At the end of each incubation period, cells were incubated with MTT agent (5 mg·mL1) at 37 ˚C for 4 h. Subsequently, the media was removed and DMSO was added to each well. The optical density was measured at the wavelength of 570 nm using a microplate reader. The untreated cells were used as a negative control, the cells treated with 1% Triton X-100 were used as a positive control. The relative growth rate (RGR) of cells was calculated using following equation:

$$RGR(\%) = \frac{OD_S - OD_P}{OD_N - OD_P} \times 100\% \quad (2)$$

Where ODS is the optical density of the samples (silicon wafer, DLC films deposited wafer), ODN is the optical density of the negative control, ODP is the optical density of positive control.

2.7. Characterizations

The Raman analyses were conducted using a confocal micro-Raman spectrometer (LabRAM-Aramis, HORIBA JobinYvon) with 532 nm frequency Ar ion laser. The XPS measurements were carried out using an X-ray photoelectron spectroscopy (ThermoFisher Scientific, ESCALAB 250Xi) with 1486.7 eV Al Kα excitation source and the results were then calibrated by the C1s peak at 285 eV. The C–C sp2/sp3 bonds fraction was calculated from the ratio between the Gaussian fitting curve areas of XPS spectra by removing the Shirley-type background. The surface morphology of the DLC film was observed by a field

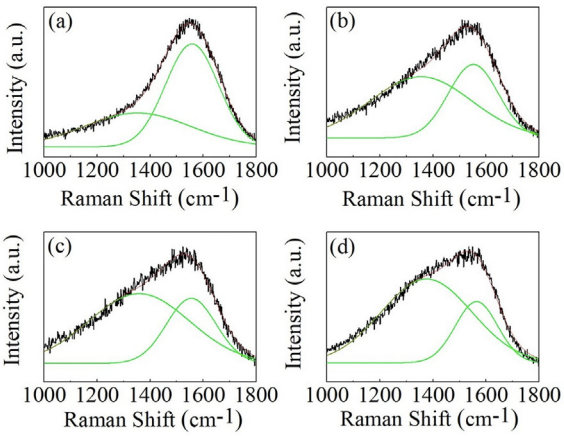

Fig. 1. Raman spectra with D and G fitting curves for the DLC films obtained using different N_2 flow rate: (a) 0 sccm; (b) 5 sccm; (c) 10 sccm; (d) 20 sccm.

emission scanning electron microscope (JEOL, JSM-7800F). The surface roughness and particle size of as-deposited films were observed using tapping mode atomic force microscope (AFM, CSPM5500). The crystalline structures of as-immersed were characterized using an X-ray diffractometer (Shimadzu, XRD7000) with Cu Kα radiation (λ = 1.5418 Å).

3. Results and discussion

3.1. Variation of C–C sp^2/sp^3 ratio using different N_2 flow rate

Fig. 1 presents the Raman spectra of the samples deposited with different N_2 flow rate from 0 to 20 sccm. All the spectra could be dominantly deconvoluted by two family bands: one band appeared at approximately 1550 cm^{-1} was ascribed to G band, corresponding to the vibration of the sp^2 bond stretching mode in the chains and rings of the carbon atoms; another peak appeared at approximately 1350 cm^{-1} was ascribed to D band and could be related to the vibrational in-plane breathing modes of sp^2 carbon atoms in the rings [23,24]. Thus, the sp^2/sp^3 ratio could be characterized by the position and width of G band and the I_D/I_G ratio, which decreased with an increase of sp^3 fraction in the amorphous carbon films [25]. Table 1 presents the parameters of the Raman spectra that can be deconvoluted into D and G bands using Gaussian function for as-deposited DLC films. The I_D/I_G ratio increased from 0.33 to 1.37 with an increase of N_2 flow rate, indicating that the increase in N_2 would benefit in forming sp^2 phase and revealing the graphitic characteristics of DLC films [26]. Furthermore, the broadening of full-width half maximum (FWHM) of G peak corresponding to the structure disorder and amorphization degree of the films [27], indicated the same evolution of an increase of sp^2 clusters. It was also noticed that the values of the FWHM of all the as-deconvoluted G peak were more than 50 cm^{-1}, thus the size of graphite crystallites should be ≤ 1 nm [25]. In this range of crystallite size, the size of sp^2-C clusters (L_a) in the DLC films can be calculated with I_D/I_G ratio according to the following equation [28]:

$$L_a = \sqrt{I_D / cI_G} \quad (3)$$

Where c is equal to 0.55 nm^{-2} [29].

As the calculated results presented in Table 1, the La value increased with a raise of I_D/I_G ratio, indicating the formation of enlarged graphite clusters with sp^2-C units. Hence, the size of graphite clusters in the DLC films increased when the N_2 flow rate was increased.

Fig. 2(a) shows the XPS survey scan of DLC films obtained using different N_2 flow rate. The characteristic peak of N_{1s} around 399.2 eV obviously increased with the increase of N_2 flow rate. Moreover, another peak centered at 532.0 eV corresponding to absorbed oxygen was observed. Fig. 2(b) indicates the effect of N_2 flow rate on the N/C atomic ratio of DLC films calculated from survey scan. The N/C atomic ratio increased greatly from 0.01 to 0.21 with the increase of N_2 flow rate from 0 to 20 sccm. In order to understand the chemical composition and the bonding configuration, C_{1s} and N_{1s} XPS peaks were respectively deconvoluted in terms of Gaussian curves and presented in Fig. 2(c) and (d). According to literature [24,25,30–32], the C_{1s} peak of DLC films obtained without using N_2 was fitted by three Gaussians curves centered at 284.6 eV, 285eV and 285.9 eV, which were attributed to C = C sp^2,C–C sp^3, C = N or C = O sp^2.The C_{1s} peaks of DLC films obtained using 5–20 sccm of N_2 were fitted by four Gaussians curves centered at 284.6 eV, 285eV, 285.9 eV and 286.9 eV, which were assigned to C = C sp^2, C–C sp^3, C = N sp^2 and C–N sp^3 bonds. The N_{1s} speaks were fitted by two Gaussians curves centered at 398.6 eV and 400.2 eV, which were attributed to C–N sp^3 and C = N sp^2 bonds, respectively. Furthermore, the area ratio of C–C sp^2 and sp^3 fitting curves were used to determine the fraction of sp^3 bonding content in the DLC films. As shown in Table 2, sp^2/sp^3 ratio increased from 1.09 to 2.66 with a raise of N_2 flow rate, in agreement with the Raman analyses that showed an increase of I_D/I_G when the N_2 flow rate was increased. As the increase of N_2 flow rate could lead to lower ion bombardment, it subsequently weakens the formation of sp^3 carbon hybridization during deposition, thus decreases the sp^2/sp^3 ratio of DLC film.

Fig. 3 presents the surface morphology of the DLC films obtained using different N_2 flow rate from 0 to 20 sccm. As seen in Fig. 3 (a), the substrate surface was fully covered with densely distributed nanosize DLC particles. With the increase of N_2 flow rate, the surface morphology changed as the extremely small nano-DLC particles grew and transformed into cauliflower-like structures, indicating an enhancement of surface roughness, in accordance with as-calculated results from Raman spectra. Concerning the previous results, it could be concluded that the roughness and the particle size of DLC films are increased by increasing sp^2/sp^3 ratio due to a raise of N_2 flow rate. In order to determine the roughness and particle sized of as-deposited films, AFM was employed to characterize the as-deposited films. The results shown in Fig. 4 and Table 3 clearly evidenced an increase of N_2 flow rate could induce the increase of surface roughness and particle size. In other words, a raise of C–C sp^2/sp^3 ratio can benefit in increasing the surface roughness and particle size of DLC film (*c.f.* Table 3).

Table 1
Parameters obtained from Raman spectra of DLC films obtained using different N_2 flow rate.

N_2 flow rate (sccm)	D band (cm^{-1})	G band (cm^{-1})	I(D)/I(G)	FWHM of G peak	La
0	1376	1561	0.33	403.78	0.78
5	1344	1550	0.83	383.53	1.23
10	1354	1550	1.07	361.63	1.39
20	1358	1555	1.37	343.15	1.58

3.2. Influence of C–C sp^2/sp^3 ratio on the biomedical properties of DLC films

An efficient method of recognizing the mechanism of osteoinduction and evaluating the *in vitro* bioactivity of surfaces is to investigate their apatite-forming ability by soaking the samples in SBF. Fig. 5 shows the surface morphology evolution of films deposited using 0–20 sccm N2 immersed in SBF during 3–28 days. At the initial 3–7 days' immersion, only a small amount of precipitates corresponding to amorphous Ca–P are observed on the samples' surfaces [33]. With the increase of C–C sp2/sp3 ratio in DLC film (0 → 1.59–1.74), the amount of amorphous Ca–P showed a notable increase and followed by a drop of Ca–P amount when sp2/sp3 ratio was increased from 1.74 to 2.66. As the immersion

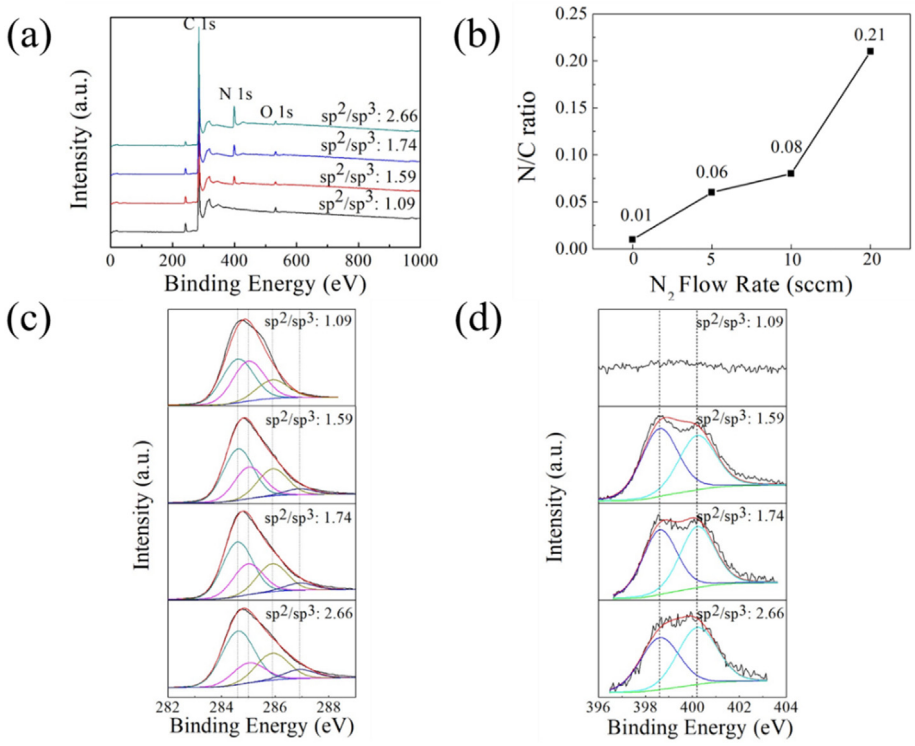

Fig. 2. XPS spectra of the DLC films obtained using different N_2 flow rate: (a) survey scan; (b) the N/C ratio varied with N_2 flow rate; (c) high resolution C_{1s}; (d) high resolution N_{1s}.

Table 2
The percentage of C,N and O of DLC films deposited using different N_2 flow rate.

N_2 flow rate (sccm)	C	N	O	sp^2	sp^3	sp^2/sp^3
	(%)	(%)	(%)	(%)	(%)	
0	92.62	0.98	6.40	42.74	39.07	1.09
5	89.61	5.05	5.34	43.85	27.56	1.59
10	86.31	7.11	6.58	45.33	26.07	1.74
20	77.95	16.25	5.80	48.91	18.42	2.66

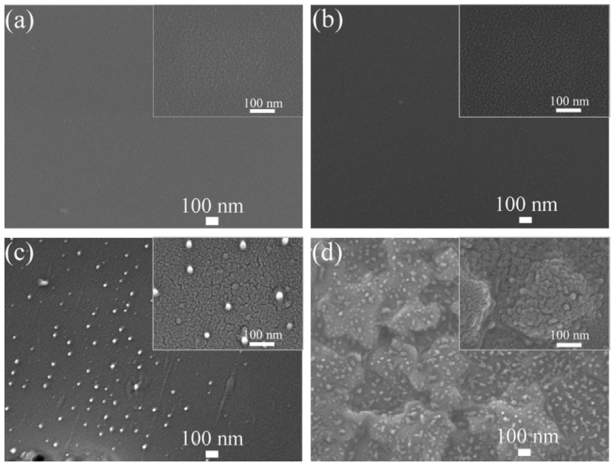

Fig. 3. Surface morphology of the DLC films obtained using different N_2 flow rate: (a) 0 sccm; (b) 5 sccm; (c) 10 sccm; (d) 20 sccm.

duration was extended to 14 days, the surfaces with different C–C sp2/sp3 ratio showed significant differences for inducing apatite. The surfaces with C–C sp2/sp3 ratio of 0–1.74 were covered with discontinuous precipitate layers, while only few ball-like particles were observed on the surface with C–C sp2/sp3 ratio of 2.66. When the immersion duration reached 28 days, the DLC films with various C–C sp2/sp3 ratio were covered with a dense apatite layer consisting of a typical urchin-like particle structure on the DLC film surfaces.

The EDS spectra of the apatite layers on the DLC films immersed for 3, 7, 14, 28 days were exhibited in Fig. 6. It can be observed that the specific peaks of Ca and P were very weak as they could not be detected at the initial stage of immersion (3 and 7 days) and the signal only comes from the Si substrate. After 14 days of immersion, the EDS spectra of the samples showed significant difference. The Ca, P peaks increased with an increment of C–C sp2/sp3 ratio from 0 to 1.74. It was also noticed that the film with the highest C–C sp2/sp3 ratio of 2.66 showed the weakest Ca, P peak intensity among all the samples. The EDS patterns of all the samples immersed for 28 days demonstrated only the specific peaks of Ca and P were obviously surveyed and the Si peak that corresponded to substrate was not detected, indicating that a thick apatite layer has covered on the surface of all the samples. Table 4 illustrated the change of Ca, P contents and the ratio of Ca/P on the surface of DLC films as a function of immersion time. It was observed distinctly the Ca and P contents on all the surface of DLC films increased with an increase of immersion duration. Especially, the increase rate of Ca (0.11 wt%→0.92 wt%→31.82 wt%) and P (0 wt%→14.37 wt%→26.38 wt%) contents of the film with C–C sp2/sp3 ratio of 1.74 was the highest among all samples. After a long-term immersion (14–28 days), the Ca/P ratios of all the surfaces are around 1.7, corresponding to that of human bones [34].

The results indicated that C–C sp2/sp3 ratio of 1.74 leads to the best coverage and growth rate of apatite. Actually, the existence of sp2 hybridization would result in the delocalization of π electron and subsequently increase the conductivity of DLC film [35]. Moreover, the increase of sp2 bond can lead to a significant raise of unpair electrons on surface, presenting a negative zeta potential [36]. As a consequence, the higher negative charged surface benefits in the attachment of Ca2+ from SBF for forming apatite. That's the reason why film's apatite

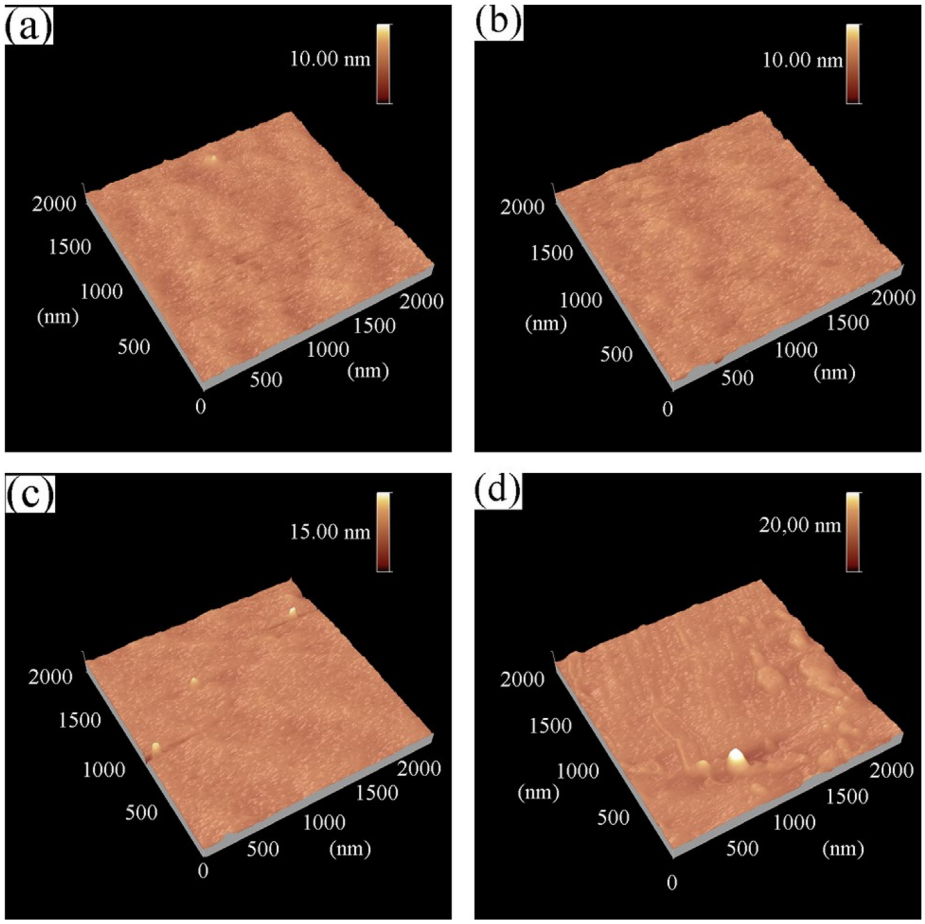

Fig. 4. AFM images of the DLC films obtained using different N_2 flow rate: (a) 0 sccm; (b) 5 sccm; (c) 10 sccm; (d) 20 sccm.

Table 3
The particle size and RMS roughness of DLC films obtained using different N_2 flow rate.

N_2 flow rate (sccm)	sp^2/sp^3 ratio	Particle size (nm)	RMS (nm)
0	1.09	43.14	0.40
5	1.59	46.59	0.44
10	1.74	58.33	0.50
20	2.66	69.78	1.08

inducing ability enhances with the increase of C–C sp2/sp3 ratio until 1.74. However, the negative charge of surface cannot be continuously increased by increasing the sp2/sp3 ratio. According to Li et al., the zeta potential of surface decreases first and then increases with a raise of C–C sp2/sp3 ratio [37]. As a result, the DLC film's apatite inducing ability would be reduced when the sp2/sp3 is changed from 1.74 to 2.66.

In order to investigate the apatite inducing ability, the corresponding X-ray diffraction patterns were recorded for samples immersed in simulated body fluid after 3–28 days, as shown in Fig. 7(a)~(d). In Fig. 7(a)~(c), all XRD patterns were similar, implying very few apatites are formed at the early immersion time of 3–14 days. After immersed for 28 days, three additional peaks at 25.9°, 31.8°, 53.1° were detected in Fig. 7(d), which could be related to the characteristic peaks of apatite, confirming the deposition of apatite on all the samples surfaces.

Samples immersed for 14 and 28 days were further measured by the XPS. The high resolution XPS spectra of Ca 2p and P 2p obtained from the surface of the DLC films were showed in Fig. 8(a) and (b). It was obviously seen that the spectra from all the sample with different C–C sp2/sp3 ratio were almost the same, which means the similar chemical structure of Ca–P matters are obtained after 14 and 28 days' immersion. DLC films with C–C sp2/sp3 ratio of 1.74 showed the best apatite inducing ability as the highest Ca, P contents were obtained for 14 days immersion. Furthermore, all the Ca 2p curves shown in Fig. 8 exhibited two deconvoluted peaks centered at 347.1 eV and 350.6 eV, corresponding to Ca 2p3/2 and Ca 2p1/2, which were attributed to the presence of Ca–O bond in apatite. Fig. 8 also showed a P2p double spectra of P2p3/2 at 132.9eV and P 2p1/2 at 133.8 eV on all the sample surfaces, corresponding to the (PO4)3- groups in the apatite structure [38,39]. The XPS results confirmed a successful formation of apatite layer on all the samples after immersion.

The hydrophilicity of DLC films with various C–C sp2/sp3 ratio were investigated through water contact angle (WCA) test. The results presented in Fig. 9 indicated a very slight hydrophilicity decrease from 77.57° to 71.71° when C–C sp2/sp3 ratio varied from 1.09 to 2.66. It was reported that WCAs around 70° could help cells to attach and proliferate on surfaces [40], thus bioactivity of DLC film surfaces is slightly enhanced with the increase of sp2/sp3 ratio.

Table 5 shows the measured absorbance values for the untreated silicon wafers and DLC films with various C–C sp2/sp3 ratio. The absorbance values of the positive and negative control groups were 0.859 and 0.160, respectively. The absorbance values of the sample surfaces significantly were changed after DLC film deposition (0.249 → 0.161–0.167). In comparison with the hemolysis rate (12.73%) of the untreated silicon wafer, the hemolysis rate of DLC deposited samples were all lower than 1%. It indicated the N doping DLC film could improve the anti-hemolysis performance of the samples and fulfill the hemolysis rate requirements for biomedical materials. With the increase of C–C sp2/sp3 ratio, hemolysis rate showed an increase from 0.14% to

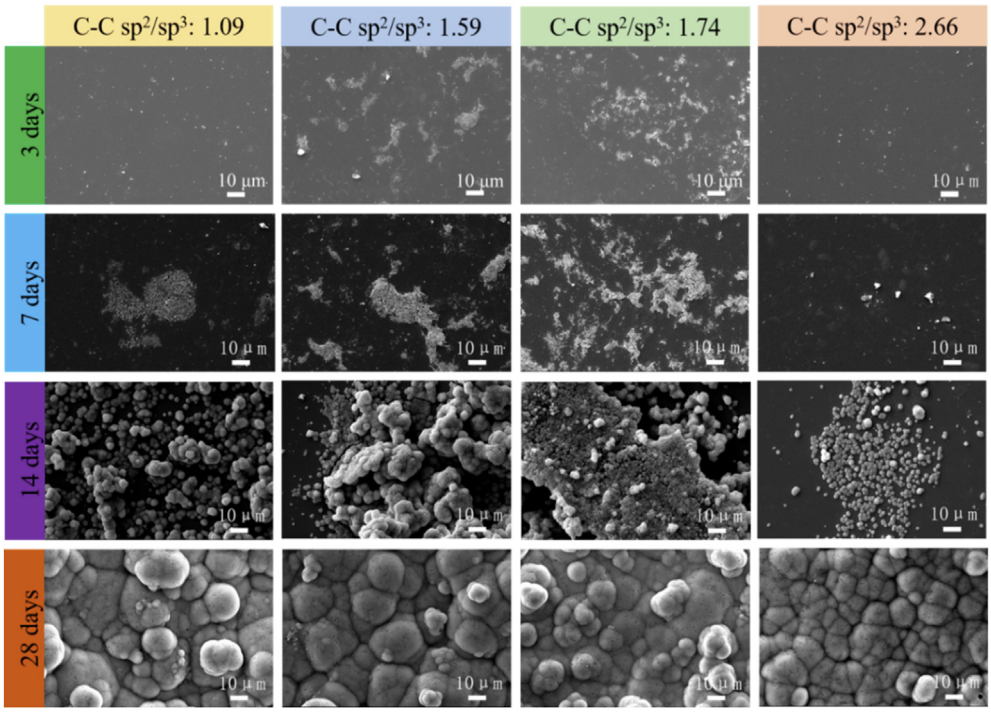

Fig. 5. SEM images of DLC films with various C–C sp^2/sp^3 ratios immersed in SBF for 3days; 7 days; 14 days and 28 days.

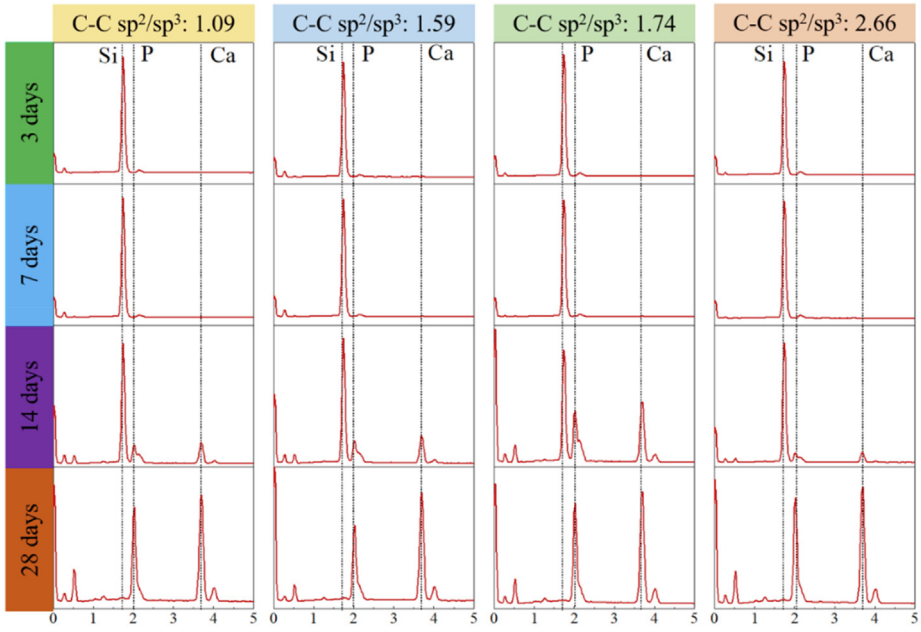

Fig. 6. EDS spectra of DLC films with various C–C sp^2/sp^3 ratios immersed in SBF for 3days; 7 days; 14 days and 28 days.

Table 4
The Ca, P contents and the Ca/P ratio of DLC films with various C–C sp^2/sp^3 ratio immersed in SBF for3, 7, 14 and 28 days.

Immersion Time	sp^2/sp^3 ratio											
	1.09			1.59			1.74			2.66		
	Ca (at%)	P (at%)	Ca/P	Ca (at%)	P (at%)	Ca/P	Ca (at%)	P (at%)	Ca/P	Ca (at%)	P (at%)	Ca/P
3 d	0.01	0	–	0.11	0	–	0.03	0	–	0.02	0	–
7 d	0.15	0	–	0.92	0	–	0.57	0	–	0.03	0	–
14 d	3.41	2.18	1.56	16.85	9.82	1.72	6.80	3.98	1.71	5.89	3.57	1.65
28 d	35.89	21.94	1.64	36.49	22.57	1.62	40.05	21.44	1.87	35.30	21.02	1.68

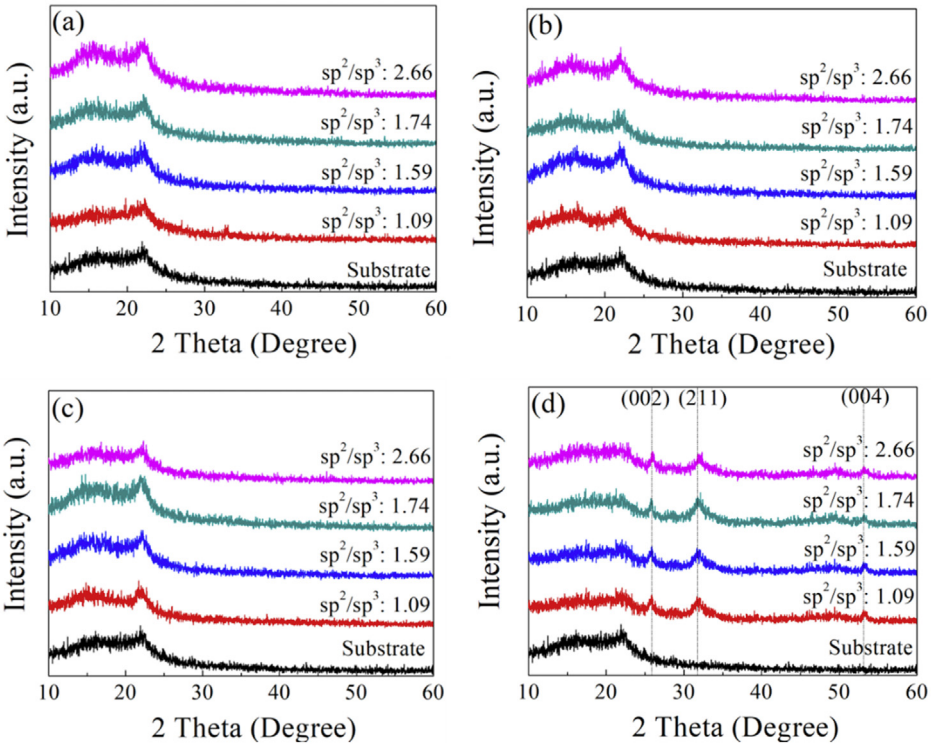

Fig. 7. XRD patterns of DLC films with various C–C sp^2/sp^3 ratios immersed in SBF for different duration: (a) 3 days; (b) 7 days; (c) 14 days; (d) 28 days.

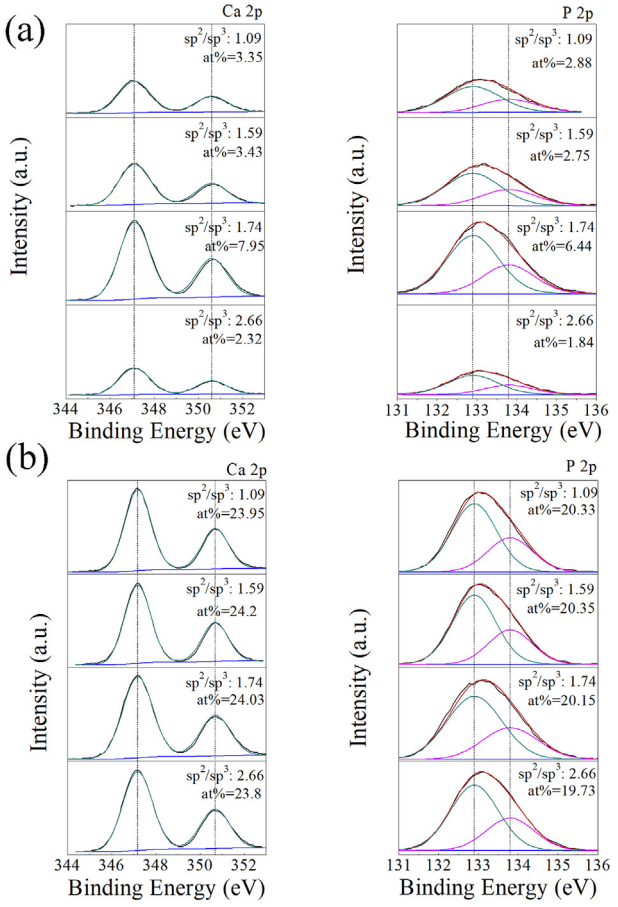

Fig. 8. High resolution XPS spectra of DLC film with various C–C sp^2/sp^3 ratios immersed in SBF for (a) 14 days and (b) 28 days.

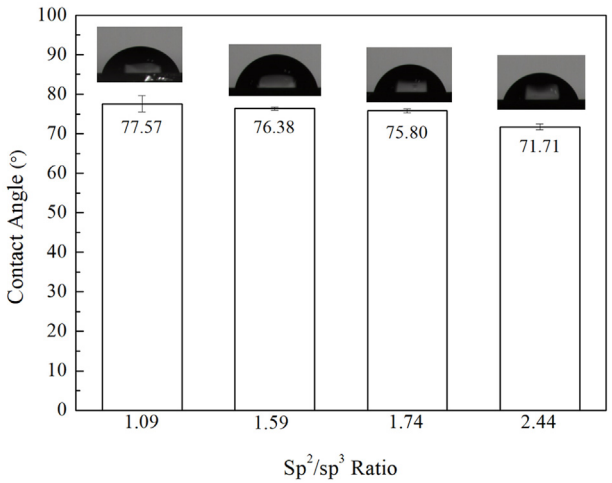

Fig. 9. Water contact angle of DLC films with different C–C sp^2/sp^3 ratio.

Table 5
Absorbance value of erythrocyte and hemolysis rate for the untreated Si and DLC films with various C–C sp^2/sp^3 ratio.

Samples	Absorbance	Hemolysis rate (%)
Negative control	0.157	–
Positive control	0.863	–
Si	0.251	13.31 ± 1.65%
sp^2/sp^3: 1.09	0.161	0.57 ± 0.12%
sp^2/sp^3: 1.59	0.162	0.71 ± 0.35%
sp^2/sp^3: 1.74	0.163	0.85 ± 0.47%
sp^2/sp^3: 2.66	0.167	1.42 ± 0.81%

1%, indicating a reduction of erythrocytes destruction.

Fig. 10 shows RGR values of HEK293T cells and cytotoxicity after culture for 1, 3 and 7 days on the surfaces of untreated silicon wafers and DLC films with various C–C sp2/sp3 ratios. On the first day of

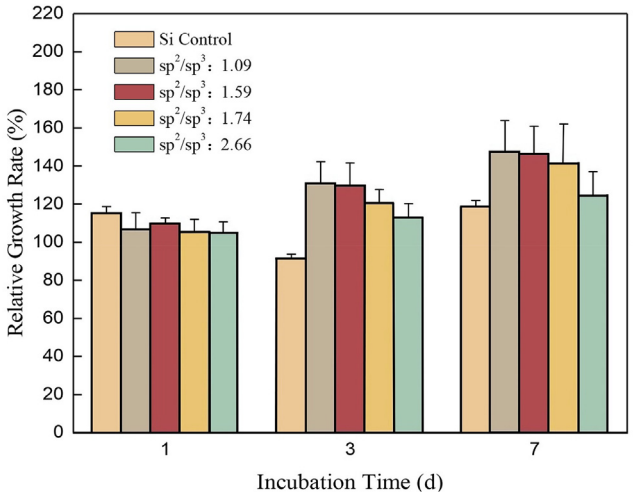

Fig. 10. The RGR of DLC films with various C–C sp2/sp3 ratios.

incubation, no obvious differences were observed as the RGRs on various DLC surfaces were around 105%. With the incubation time increasing to 3 and7 days, the DLC films with different C–C sp^2/sp^3 ratio exhibited RGRs variation. The number of HEK293T cells decreased with the increase of C–C sp^2/sp^3 ratio, indicating a reduction of biocompatibility. It was also noticed that all the RGRs on various DLC films were always higher than 100% during 1–7 days' incubation, indicating the cytotoxicity level of all the as-deposited DLC film was 0. The results evidenced the DLC films fabricated in our FCVA system has no harm to the cells.

3.3. Influence of C–C sp^2/sp^3 ratio on the tribological property of DLC films

The friction coefficients of DLC films in ambient air and SBF lubrication were presented in Fig. 11. The friction coefficient of all the surfaces was effectively reduced after the DLC film deposition, indicating the DLC film is promising for enhancing joint implants. In comparison, the friction coefficient of DLC films was lower than that in ambient air. It is probably due to the formation of the continuous SBF solution layer on the mating surface, which divides the friction contact faces and inhibits the effect of friction contact faces on the friction behavior. In ambient air, the friction coefficient of the as-deposited DLC film increased as the C–C sp2/sp3 was increased from 1.09 to 2.66 (Fig. 11(a)). In SBF lubrication, the friction coefficient of DLC films exhibited the same evolution (Fig. 11(b)). Actually, the increase of C–C sp2/sp3 ratio means a raise of sp2 clusters and/or the decrease of structure disorder and the amorphization degree, resulting in the formation of the carbonaceous transferred-layer on the mated surfaces [27]. It could reduce the friction coefficient of film surface, which is however contrary to our results. Generally, materials with a lower elastic modulus are less resistant to stress that would result in a larger real contact area under a given load [41]. The elastic modulus is reported to decrease with the increase of the N2 flow rate [42], which effectively causes the raise of contact area, and subsequently increases the friction resistance of DLC films. In other words, the increase of C–C sp2/sp3 ratio in this work leads to a higher friction coefficient. Moreover, the decrease of smoothness and increase of roughness (*c.f.* Figs. 3 and 4) also lead to the slight increase of the friction coefficient.

4. Conclusions

DLC films were successfully fabricated by a filtered cathodic vacuum arc system. The C–C sp2/sp3 ratio increased from 1.09 to 2.66 with the increase of N2 flow rate from 0 to 20sccm. The SBF immersion results showed that the DLC films with different C–C sp2/sp3 ratio were very promissory to improve of the apatite formation in 28 days. The C–C sp2/sp3 ratio enhanced the apatite formation with the increase of C–C sp2/sp3 ratio from 1.09 to 1.74 and then reduces a little due to the surface charge effect. The WCAs of the DLC film surfaces were in the range of 77.57°~71.71°, implying as-fabricated films favored the attachment and proliferation of cells. All the DLC films showed good antihemolysis of < 1% and low cytotoxicity level of 0. The increase of C–C sp^2/sp^3 ratio also resulted in a slight decrease in hemolysis rate and RGRs, indicating a tiny negative effect on the biocompatibility of DLC films. Tribological results proved DLC films reduce the friction coefficient in air and in SBF lubrication environment. The friction coefficient increased by increasing C–C sp^2/sp^3 ratio, as a result of raising contact area on mated surfaces.

CRediT authorship contribution statement

Xi Rao: Conceptualization, Methodology, Writing - original draft. **Jihan Yang:** Investigation, Validation, Formal analysis, Visualization, Software. **Zilin Chen:** Validation, Formal analysis, Visualization. **Yidie Yuan:** Data curation. **Qiubing Chen:** Data curation. **Xue Feng:** Writing - review & editing. **Lizhao Qin:** Resources. **Yongping Zhang:** Validation, Writing - review & editing, Supervision.

Declaration of competing interest

The authors declare that they have no known competing financial interests or personal relationships that could have appeared to influence the work reported in this paper.

Acknowledgment

The authors acknowledge support from National Natural Science Foundation of China (Grant 51801164). Besides, this work is jointly supported by Fundamental Research Funds for the Central Universities (Grant XDJK2020C005), National Training Program of Innovation and Entrepreneurship for Undergraduates (Grant 201810635068) and the

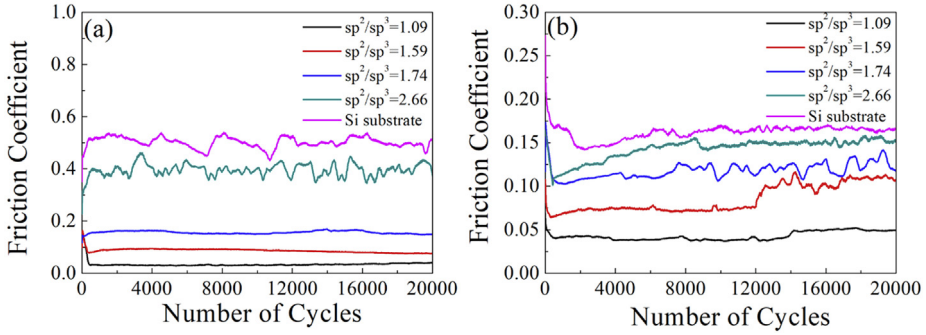

Fig. 11. The friction coefficient of DLC films with various C–C sp2/sp3 ratios under different conditions: (a) ambient air, (b) SBF lubrication.

Venture & Innovation Support Program for Chongqing Overseas Returnees (Grant cx2018080).

References

[1] A.J. Smith, P. Dieppe, M. Porter, A.W. Blom, Risk of cancer in first seven years after metal-on-metal hip replacement compared with other bearings and general population: linkage study between the national joint registry of england and wales and hospital episode statistics, Br. Med. J. 344 (2012) e2383.

[2] S.M. Kurtz, J.M. Toth, R. Siskey, L. Ciccarelli, D. Macdonald, J. Isaza, T. Lanman, I. Punt, M. Steinbeck, J. Goffin, A. van Ooij, The latest lessons learned from retrieval analyses of ultra-high molecular weight polyethylene, metal-on-metal, and alternative bearing total disc replacements, Semin. Spine Surg. 24 (2012) 57–70.

[3] H. Maradit Kremers, D.R. Larson, C.S. Crowson, W.K. Kremers, R.E. Washington, C.A. Steiner, W.A. Jiranek, D.J. Berry, Prevalence of total Hip and knee Replacement in the United States, J. Bone Joint Surg. Am. 97 (2015) 1386–1397.

[4] J. Huang, L. Wang, B. Liu, S. Wan, Q. Xue, In vitro evaluation of the tribological response of Mo-doped graphite-like carbon film in different biological media, ACS Appl. Mater. Interfaces 7 (2015) 2772–2783.

[5] W.-H. Liao, C.-R. Lin, D.-H. Wei, Y.-R. Shen, Y.-C. Li, J.-A. Lee, C.-Y. Liang, Concurrent improvement in biocompatibility and bioinertness of diamond-like carbon films with nitrogen doping, J. Biomed. Mater. Res. 100A (2012) 3151–3156.

[6] B.C. Ramos, E. Saito, V.J. Trava-Airoldi, A.O. Lobo, F.R. Marciano, Diamond-like carbon electrochemical corrosion resistance by addition of nanocrystalline diamond particles for biomedical applications, Surf. Coating. Technol. 259 (2014) 732–736.

[7] K. Sakurai, M. Hiratsuka, H. Nakamori, K. Namiki, K. Hirakuri, Evaluation of sliding properties and durability of DLC coating for medical devices, Diam. Relat. Mater. 96 (2019) 97–103.

[8] G. Gotzmann, J. Beckmann, B. Scholz, U. Herrmann, C. Wetzel, Low-energy electron-beam modification of DLC coatings reduces cell count while maintaining biocompatibility, Surf. Coating. Technol. 336 (2018) 34–38.

[9] D. Bociaga, A. Sobczyk-Guzenda, W. Szymanski, A. Jedrzejczak, A. Jastrzebska, A. Olejnik, K. Jastrzebski, Mechanical properties, chemical analysis and evaluation of antimicrobial response of Si-DLC coatings fabricated on AISI 316 LVM substrate by a multi-target DC-RF magnetron sputtering method for potential biomedical applications, Appl. Surf. Sci. 417 (2017) 23–33.

[10] W. Yang, Y. Gao, D. Xu, J. Zhao, P. Ke, A. Wang, Bactericidal abilities and in vitro properties of diamond-like carbon films deposited onto MAO-treated titanium, Mater. Lett. 244 (2019) 155–158.

[11] J. Gutierrez Bernal, G. Capote, V. Trava-Airoldi, High antibacterial properties of DLC film doped with nanodiamond, Surf. Coating. Technol. 375 (2019) 395–401.

[12] C. Wei, K.-S. Peng, M.-S. Hung, The effect of hydrogen and acetylene mixing ratios on the surface, mechanical and biocompatible properties of diamond-like carbon films, Diam. Relat. Mater. 63 (2016) 108–114.

[13] A. Dorner-Reisel, C. Schurer, G. Irmer, F. Simon, C. Nischan, E. Muller, Diamond-like carbon coatings with Ca-O-incorporation for improved biological acceptance, Anal. Bioanal. Chem. 374 (2002) 753–755.

[14] K. Fox, J.P.R. Judge, A.D. Greentree, Diamond as a scaffold for bone growth, J. Mater. Sci. Mater. Med. 24 (2013) 849–861.

[15] F.S. Lopes, J.R. Oliveira, J. Milani, L.D. Oliveira, J.P.B. Machado, V.J. Trava-Airoldi, A.O. Lobo, F.R. Marciano, Biomineralized diamond-like carbon films with incorporated titanium dioxide nanoparticles improved bioactivity properties and reduced biofilm formation, Mater. Sci. Eng. C Mater. Biol. Appl. 81 (2017) 373–379.

[16] M.A. Al Mamun, H. Furuta, A. Hatta, Pulsed dc plasma cvd system for the deposition of dlc films, Mater. Today Commun. 14 (2018) 40–46.

[17] B.K. Tay, Z.W. Zhao, D.H.C. Chua, Review of metal oxide films deposited by filtered cathodic vacuum arc technique, Mater. Sci. Eng. R Rep. 52 (2006) 1–48.

[18] M.A. Rahman, P. Maguire, S.S. Roy, R. McCann, F. McKavanagh, J.A. McLaughlin, *Sp^3 Content in Ta-C films vs pulse bias Width to the substrate: a correlative structural analysis*, Diam. Relat. Mater. 18 (2009) 1343–1347.

[19] J. Corona-Gomez, S. Shiri, M. Mohammadtaheri, Q. Yang, Adhesion enhancement of dlc on CoCrMo alloy by diamond and nitrogen incorporation for wear resistant applications, Surf. Coating. Technol. 332 (2017) 120–127.

[20] D. Bootkul, B. Supsermpol, N. Saenphinit, C. Aramwit, S. Intarasiri, Nitrogen doping for adhesion improvement of DLC film deposited on Si substrate by filtered cathodic vacuum arc (FCVA) technique, Appl. Surf. Sci. 310 (2014) 284–292.

[21] X. Shi, B.K. Tay, H.S. Tan, E. Liu, J. Shi, L.K. Cheah, X. Jin, Transport of vacuum arc plasma through an off-plane double bend filtering duct, Thin Solid Films 345 (1999) 1–6.

[22] T. Kokubo, H. Takadama, How useful is SbF in predicting in vivo bone bioactivity? Biomaterials 27 (2006) 2907–2915.

[23] H. Wu, T. Zhou, N. Zhang, X. Zhu, Assessments of the relation between the degree of order of the ultrafast laser deposited carbon film and the features of the Raman spectrum's D band, Surf. Coating. Technol. 311 (2017) 55–62.

[24] A. Hatem, J. Lin, R. Wei, R.D. Torres, C. Laurindo, P. Soares, Tribocorrosion behavior of DLC-coated Ti-6Al-4V alloy deposited by PIID and PEMS + PIID techniques for biomedical applications, Surf. Coating. Technol. 332 (2017) 223–232.

[25] M. Qi, J. Xiao, Y. Cheng, Z. Wang, A. Jiang, Y. Guo, Z. Tao, Effect of various nitrogen flow ratios on the optical properties of (Hf:N)-DLC films prepared by reactive magnetron sputtering, AIP Adv. 7 (2017) 085012.

[26] Z. Gong, J. Shi, B. Zhang, J. Zhang, Graphene nano scrolls responding to superlow friction of amorphous carbon, Carbon 116 (2017) 310–317.

[27] T. Chen, X. Wu, Z. Ge, J. Ruan, B. Lv, J. Zhang, Achieving low friction and wear under various humidity conditions by Co-doping nitrogen and silicon into diamond-like carbon films, Thin Solid Films 638 (2017) 375–382.

[28] B. Zhou, Z. Liu, D.G. Piliptsou, S. Yu, Z. Wang, A.V. Rogachev, A.S. Rudenkov, A. Balmakou, Structure and optical properties of Cu-DLC composite films deposited by cathode arc with double-excitation source, Diam. Relat. Mater. 69 (2016) 191–197.

[29] F. Sohbatzadeh, M. Eshghabadi, T. Mohsenpour, Controllable synthesizing DLC nano structures as a super hydrophobic layer on cotton fabric using a low-cost ethanol electrospray-assisted atmospheric plasma jet, Nanotechnology 29 (2018) 265603.

[30] W. Dai, S.-H. Kwon, Q. Wang, J. Liu, *Influence of Frequency and C_2H_2 Flow on growth Properties of diamond-like carbon Coatings with AlCrSi Co-doping deposited Using a reactive high power impulse magnetron sputtering*, Thin Solid Films 647 (2018) 26–32.

[31] Z. Seker, H. Ozdamar, M. Esen, R. Esen, H. Kavak, The effect of nitrogen incorporation in DLC films deposited by ECR microwave plasma CVD, Appl. Surf. Sci. 314 (2014) 46–51.

[32] Q. Wang, X. Chang, Y. Kikuchi, K.Y. Inoue, T. Kubota, T. Matsue, T. Nozawa, S. Samukawa, Structure and electrochemical properties of nitrogen doped diamond-like carbon film synthesized by low temperature neutral beam enhanced chemical vapor deposition, Int. J. Electrochem. Sci. 13 (2018) 1803–1812.

[33] D. Wei, Y. Zhou, Y. Wang, Q. Meng, D. Jia, *Structure and apatite Formation of microarc oxidized TiO_2-based Films before and after alkali-Treatment by various alkali concentrations*, Surf. Coating. Technol. 202 (2008) 5012–5019.

[34] S.V. Dorozhkin, Calcium orthophosphates, J. Mater. Sci. 42 (2007) 1061–1095.

[35] D.S. Su, S. Perathoner, G. Centi, Nanocarbons for the development of advanced catalysts, Chem. Rev. 113 (2013) 5782–5816.

[36] S.S. Li, B.J. Wu, Q.Y. Deng, Y.B. Guo, Y.X. Leng, N. Huang, *In vitro cytotoxicity Evaluation of nano-carbon Particles with different sp^2/sp^3 ratios*, Mater. Sci. Eng. C Mater. Biol. Appl. 75 (2017) 854–862.

[37] C. Hai, M. Fuji, H. Watanabe, F. Wang, T. Shirai, M. Takahashi, Evaluation of surfactant-free stabilized vapor grown carbon fibers with zeta-potential and Raman spectroscopy, Colloid. Surface. Physicochem. Eng. Aspect. 381 (2011) 70–73.

[38] D. Li, Y. Gong, X. Chen, B. Zhan, H. Zhang, P. Jin, H. Li, Room-temperature deposition of hydroxyapatite/antibiotic composite coatings by vacuum cold spraying for antibacterial applications, Surf. Coating. Technol. 330 (2017) 87–91.

[39] Z. Song, Y. Liu, J. Shi, T. Ma, Z. Zhang, H. Ma, S. Cao, Hydroxyapatite/mesoporous silica coated gold nanorods with improved degradability as a multi-responsive drug delivery platform, Mater. Sci. Eng. C Mater. Biol. Appl. 83 (2018) 90–98.

[40] M.M. Gentleman, E. Gentleman, The role of surface free energy in osteoblast-biomaterial interactions, Int. Mater. Rev. 59 (2014) 417–429.

[41] D. Dong, B. Jiang, H. Li, Y. Du, C. Yang, Effect of graphite target power density on tribological properties of graphite-like carbon films, Appl. Surf. Sci. 439 (2018) 900–909.

[42] S.R. Polaki, K. Ganesan, S.K. Srivastava, M. Kamruddin, A.K. Tyagi, The role of substrate bias and nitrogen doping on the structural evolution and local elastic modulus of diamond - like carbon films, J. Phys. D Appl. Phys. 50 (2017) 175601.